

# ISAR IMAGING OF MANEUVERING TARGETS VIA MATCHING PURSUIT

*Gang Li<sup>+</sup>, Hao Zhang<sup>+</sup>, Xiqin Wang<sup>+</sup>, and Xiang-Gen Xia<sup>++</sup>*

<sup>+</sup> Department of Electronic Engineering, Tsinghua University, China

<sup>++</sup> Department of Electrical and Computer Engineering, University of Delaware, USA

## 1. INTRODUCTION

Inverse synthetic aperture radar (ISAR) is an effective tool to acquire high resolution images of maneuvering targets such as aircrafts and ships. A kind of promising methods of ISAR imaging are based on time-frequency techniques [2-5], especially the parametric time-frequency techniques [3-5]. In [3-5], the ISAR signal is adaptively decomposed and parameterized as a summation of some basis chirplet or Gaussian functions that best represent the time-frequency characteristic of the ISAR signal. By selecting correct basis functions via the matching pursuit (MP) technique, the phase parameters can be determined, and then the image focusing is accomplished by first eliminating the high order phase error and then performing Fourier transform. It is noted that the common step of image focusing in most of the above algorithms is Fourier transform, so the imaging results have to suffer from the inherent problem of Fourier transform such as low resolution and the high sidelobe.

In this paper, we propose a new algorithm of ISAR imaging via MP technique. Assume that the rotation rate of the target is constant during short observation duration. Given a target rotation rate, we decompose an ISAR signal as a summation of many basis sub-signals that are generated by discretizing the target spatial domain and synthesizing the ISAR data for every discretized spatial position. The ISAR imaging problem is converted into the problem of selection of basis sub-signals. Since in ISAR application the target spatial domain is sparse, i.e., the number of dominant scatterers is much smaller than the number of discretized spatial positions, the selection of correct basis sub-signals can be implemented by the improved MP technique [6]. Then the projection coefficients of the ISAR echo on the selected basis sub-signals directly represent the ISAR image. In the case that the target rotation rate is not known in prior, the true rotation rate of the target is determined by searching a rotation rate candidate such that the contrast of corresponding ISAR image candidate reaches the maximum.

It should be emphasized that here the MP technique is employed in a different way from [3-5]. In [3-5] the chirplet or Gaussian functions are chosen as the basis functions, and MP solution is used to accurately estimate the signal phase parameters and remove the high order phase error, but the image focusing is implemented via Fourier transform. The proposed algorithm designs specific basis sub-signals such that the MP solution directly represents the ISAR final image (including the positions and the reflectivities of all scatterers), so the advantages of the MP such as high resolution and low sidelobe [6] indeed improve the image quality.

## 2. FORMULATION OF PROPOSED ALGORITHM

Assume the translational motion compensation has been done as [1] and consider the scenario that the target is uniformly rotating as shown in Fig. 1. We discretize the target spatial domain as  $K \times L$  positions, where  $K$  is the number of range bins and  $L$  is the number of cross-range bins. If a scatterer with the reflectivity 1 is located at spatial coordinates  $(k, l)$ , the instantaneous range migration of this scatterer can be written as [1-5]

$$r_{k,l}(t; \omega_0) = l\rho_x \sin(\omega_0 t) + k\rho_y \cos(\omega_0 t) \quad (1)$$

where  $t$  is the slow time,  $\omega_0$  is the rotation rate of the target that can be considered constant during the short observation duration,  $\rho_x$  and  $\rho_y$  are the cross-range and range resolutions determined by the discretization level/grid of the target spatial domain. Thus the ISAR echo from this scatterer can be expressed as

$$s_{k,l}(\tau, t; \omega_0) = a\left(\tau - \frac{r_{k,l}(t; \omega_0)}{2c}\right) \cdot \exp\left[-j\frac{4\pi}{\lambda}r_{k,l}(t; \omega_0)\right], \quad (2)$$

where  $\tau$  is the fast time,  $c$  is the speed of light,  $a(\cdot)$  denotes the range signal profile,  $\lambda$  is the radar wavelength.

Firstly, we assume that the rotation rate of the target  $\omega_0$  is known. By discretizing  $\tau$  and  $t$  as  $\tau = [1, 2, \dots, M]/F_s$  and  $t = [1, 2, \dots, N]/F_p$ , respectively, where  $F_s$  is the radar sampling rate and  $F_p$  is the pulse repetition frequency, the discrete form of (2) can be described as a  $M \times N$  matrix  $\mathbf{S}_{k,l}$  whose  $(m, n)$ th element is

$$\mathbf{S}_{k,l}(m, n; \omega_0) = a\left(\frac{m}{F_s} - \frac{1}{2c} \cdot r_{k,l}\left(\frac{n}{F_p}; \omega_0\right)\right) \cdot \exp\left[-j\frac{4\pi}{\lambda}r_{k,l}\left(\frac{n}{F_p}; \omega_0\right)\right], \quad (3)$$

$m = 1, 2, \dots, M$ ,  $n = 1, 2, \dots, N$ . From (3) one can see that  $\mathbf{S}_{k,l}$  is dependent on the spatial position  $(k, l)$  that indicates the position of the scatterer in the discretized spatial domain. Thus the projection of the ISAR echo on all of  $\mathbf{S}_{k,l}$  can reflect the target spatial domain. We define the vectorization of  $\mathbf{S}_{k,l}$  (the result is denoted by  $\mathbf{S}_{k,l}^{\text{vec}}$ ) as a sub-signal corresponding to the spatial position  $(k, l)$ . Here the vectorization of  $\mathbf{S}_{k,l}$  is carried out by stacking the columns of  $\mathbf{S}_{k,l}$  one underneath the other in sequence, i.e, the  $MN \times 1$  sub-signal  $\mathbf{S}_{k,l}^{\text{vec}}$  is generated by

$$\mathbf{S}_{k,l}^{\text{vec}} \triangleq \left[ \underbrace{\mathbf{S}_{k,l}(1,1), \mathbf{S}_{k,l}(2,1), \dots, \mathbf{S}_{k,l}(M,1)}_{\text{1st column of } \mathbf{S}_{k,l}}, \underbrace{\mathbf{S}_{k,l}(1,2), \mathbf{S}_{k,l}(2,2), \dots, \mathbf{S}_{k,l}(M,2)}_{\text{2nd column of } \mathbf{S}_{k,l}}, \dots, \underbrace{\mathbf{S}_{k,l}(1,N), \mathbf{S}_{k,l}(2,N), \dots, \mathbf{S}_{k,l}(M,N)}_{\text{Nth column of } \mathbf{S}_{k,l}} \right]^T, \quad (4)$$

where  $(\cdot)^T$  denotes the transpose operation. For  $k = 1, 2, \dots, K$  and  $l = 1, 2, \dots, L$ , we generate  $KL$  sub-signals that respectively correspond to all discretized spatial positions, and we stack them as a  $MN \times KL$  matrix  $\Phi(\omega_0)$ :

$$\Phi(\omega_0) \triangleq \left[ \mathbf{S}_{1,1}^{\text{vec}}, \mathbf{S}_{2,1}^{\text{vec}}, \dots, \mathbf{S}_{K,1}^{\text{vec}}, \mathbf{S}_{1,2}^{\text{vec}}, \mathbf{S}_{2,2}^{\text{vec}}, \dots, \mathbf{S}_{K,2}^{\text{vec}}, \dots, \mathbf{S}_{1,L}^{\text{vec}}, \mathbf{S}_{2,L}^{\text{vec}}, \dots, \mathbf{S}_{K,L}^{\text{vec}} \right]. \quad (5)$$

Thus the received ISAR echo  $\mathbf{x}$  can be expressed as

$$\mathbf{x} = \sum_{k=1}^K \sum_{l=1}^L \mathbf{S}_{k,l}^{\text{vec}} \cdot \theta_{k,l} = \Phi(\omega_0) \cdot \boldsymbol{\theta}, \quad (6)$$

where  $\mathbf{x}$  is a  $MN \times 1$  vector,  $\boldsymbol{\theta} = [\theta_{1,1}, \theta_{2,1}, \dots, \theta_{K,1}, \theta_{1,2}, \theta_{2,2}, \dots, \theta_{K,2}, \dots, \theta_{1,L}, \theta_{2,L}, \dots, \theta_{K,L}]^T$  is a sparse  $KL \times 1$  vector indicating the complex reflectivities at all discretized spatial positions. Thus the ISAR imaging problem is converted into solving  $\boldsymbol{\theta}$  from the measurement vector  $\mathbf{x}$  with a pre-designed sub-signal dictionary  $\Phi(\omega_0)$ . This can be implemented via the modified MP technique [6]:

$$\text{minimize } \|\boldsymbol{\theta}\|_1 \quad \text{subject to } \|\mathbf{x} - \Phi(\omega_0) \cdot \boldsymbol{\theta}\|_2 \leq \varepsilon, \quad (7)$$

where  $\|\cdot\|_1$  and  $\|\cdot\|_2$  denotes  $\ell_1$  and  $\ell_2$  norms, respectively,  $\varepsilon$  is the error threshold. Once  $\boldsymbol{\theta}$  is solved, an ISAR image of size  $K \times L$  is obtained.

In what follows, we deal with the case of unknown rotation rate of the target. Given a candidate rotation rate  $\omega$ , we create the sub-signal dictionary  $\Phi(\omega)$  according to (3)-(5) and solve (7) by replacing  $\Phi(\omega_0)$  by  $\Phi(\omega)$ , and the solution of (7) is denoted by  $\boldsymbol{\theta}(\omega)$ . Now the problem is to seek for a parameter/quantity to measure whether the  $\boldsymbol{\theta}(\omega)$  correctly represents the true target spatial domain. To do so, the concept of image contrast is used here, which is a well-known parameter evaluating the SAR image quality [7]. The contrast of  $\boldsymbol{\theta}(\omega)$  is defined as

$$C_0(\omega) = \langle \boldsymbol{\theta}(\omega)^2 \rangle / \langle \boldsymbol{\theta}(\omega) \rangle^2, \quad (8)$$

where  $\langle \cdot \rangle$  denotes the averaging operator. If the candidate  $\omega$  is equal to the true  $\omega_0$ , the solution of  $\boldsymbol{\theta}(\omega)$  presents a clear ISAR image that correctly represents the true target spatial domain, so a larger  $C_0$  is obtained. Contrarily, if the candidate  $\omega$  is apart from the true  $\omega_0$ , the solution of  $\boldsymbol{\theta}(\omega)$  presents a blurred ISAR image, so  $C_0$  becomes smaller. This implies that the  $C_0$  produced by the true  $\omega_0$  is larger than the one produced by a wrong candidate  $\omega$ . Thus, the correct rotation rate can be estimated by searching  $\omega$  such that  $C_0$  reaches the maximum.

### 3. EXAMPLES AND CONCLUSION

We use the simulated MIG-25 data [8] to verify the effectiveness of the proposed algorithm. The radar bandwidth is 512MHz that is synthesized by a pulse burst consisting of 64 stepped-frequency pulses, the pulse repetition frequency is 15kHz, the carrier frequency is 9GHz. The result of the discrete Fourier transform on 64 pulses in a burst is taken as the range signal profile  $a(\cdot)$ . To reduce the data size, the original burst repetition frequency in [8] is halved, i.e., only the pulse bursts with odd indexes are picked from the original data in [8].

Let  $M=40$ ,  $N=50$ ,  $K=80$  and  $L=100$ , i.e., 40 range samples and 50 pulse bursts are taken, and the target spatial domain are discretized as  $80 \times 100$  positions. The  $C_0$  in (8) versus different rotation rate candidate  $\omega$  is plotted in Fig. 2, where the true rotation rate of the aircraft is obtained (about  $8.5^\circ/\text{s}$ ) by finding the maximum of  $C_0$ . By substituting  $\tilde{\omega}_0 = 8.5^\circ/\text{s}$  into (3)-(5) and solving the ISAR image  $\boldsymbol{\theta}(\omega_0)$  by (7), a clear ISAR image is obtained by the proposed algorithm as shown in Fig. 3. For comparison, the imaging results of the algorithm of time-

frequency technique [4] by 100 pulse bursts are shown in Fig. 4. It is clear that, the proposed algorithm improves both range and cross-range resolutions and removes sidelobe artifacts with less data.

#### 4. REFERENCES

- [1] J. Wang and D. Kasilingam, "Global range alignment for ISAR," IEEE Transactions on Aerospace and Electronic Systems, vol. 39, no. 1, pp. 351-357, Jan. 2003.
- [2] V. C. Chen and H. Ling, Time-frequency transforms for radar imaging and signal analysis, Artech House, Boston, 2002
- [3] J. Li and H. Ling, "Application of adaptive chirplet representation for ISAR feature extraction from targets with rotating parts," IEE Proceedings - Radar Sonar & Navigation, vol. 150, no. 4, pp. 284-291, Aug. 2003.
- [4] G. Wang and Z. Bao, "Inverse synthetic aperture radar imaging of maneuvering targets based on chirplet decomposition," Optical Engineering, vol. 38, no. 9, pp. 1534-1541, Sep. 1999.
- [5] L. C. Trintinalia and H. Ling, "Joint time-frequency ISAR using adaptive processing," IEEE Transactions on Antennas and Propagation, vol. 45, no. 2, pp. 221-227, Feb. 1997.
- [6] D. Needell and R. Vershynin, "Uniform uncertainty principle and signal recovery via regularized orthogonal matching pursuit," Foundations on Computational Mathematics, vol. 9, pp. 317-334, 2009
- [7] C. Oliver and S. Quegan, Understanding synthetic aperture radar images, Norwood, MA: Artech House, 1998.
- [8] Provided by Dr. V. C. Chen. Available at: <http://airborne.nrl.navy.mil/~vchen/tftsa.html>

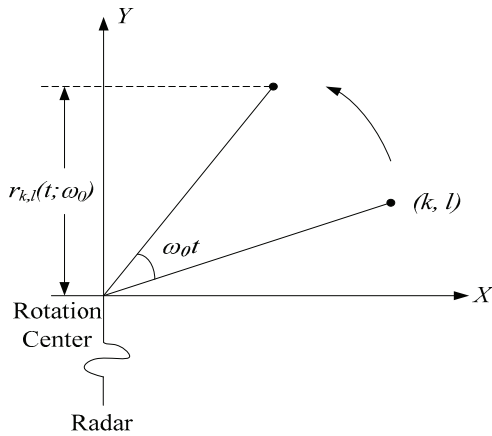


Fig. 1. The geometry of a rotating scatterer.

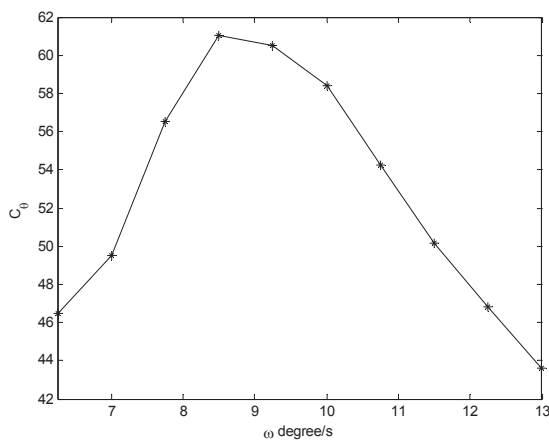


Fig. 2  $C_0$  versus different rotation rate candidate  $\omega$

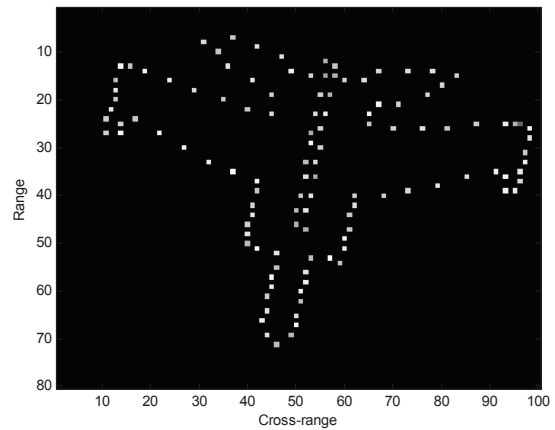


Fig. 3 Imaging results by using the proposed algorithm on 50 pulse bursts.

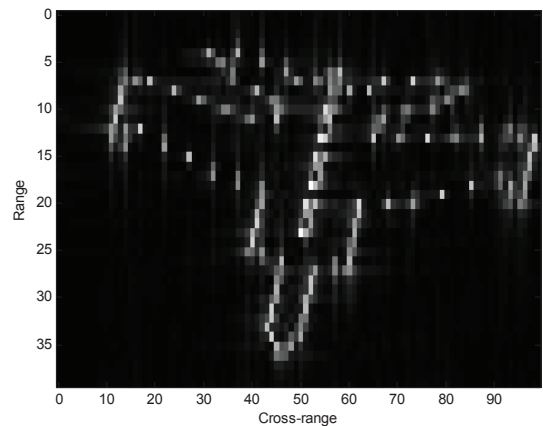


Fig. 4 Imaging results by using the chirplet decomposition algorithm on 100 pulse bursts